Single-Molecule Dissociation by Tunneling Electrons

B. C. Stipe, M. A. Rezaei, and W. Ho
Laboratory of Atomic and Solid State Physics and Materials Science Center, Cornell University, Ithaca, New York 14853

S. Gao, M. Persson, and B. I. Lundqvist
Department of Applied Physics, Chalmers University of Technology, S-412 96 Göteborg, Sweden
(Received 17 March 1997)

The tunneling current from a scanning tunneling microscope was used to image and dissociate single O_2 molecules on the Pt(111) surface in the temperature range of 40 to 150 K. After dissociation, the two oxygen atoms are found one to three lattice constants apart. The dissociation rate as a function of current was found to vary as $I^{0.8\pm0.2}$, $I^{1.8\pm0.2}$, and $I^{2.9\pm0.3}$ for sample biases of 0.4, 0.3, and 0.2 V, respectively. These rates are explained using a general model for dissociation induced by intramolecular vibrational excitations via resonant inelastic electron tunneling. [S0031-9007(97)03318-8]

PACS numbers: 61.16.Ch, 68.10.Jy, 68.35.Bs, 68.45.Kg

It has been a long-standing goal to manipulate matter atom by atom [1,2]. Over the past 10 years, the scanning tunneling microscope (STM) has raised expectations as an effective tool for the manipulation of individual atoms and molecules on surfaces [3]. For example, atoms and molecules on surfaces have been repositioned with the STM tip [4], and resonant inelastic tunneling electrons have been used to reversibly transfer a single xenon atom between the tip and a Ni(110) substrate [5] and desorb hydrogen atoms from a single dimer row of the Si(100)-(2 × 1) surface [6]. By scanning regions of the Si(111)-(7 × 7) surface with the sample biased at ≥4 V, the dissociation of adsorbed $B_{10}H_{14}$ molecules into a variety of fragments was observed due to the dose of electrons from the STM tip [7]. After scanning regions of the same surface with the sample biased at ≥6 V, the dissociation of adsorbed O_2 molecules was observed by resonant electron capture in unoccupied O_2 energy levels [8].

Here, we report the ability to induce a particular unimolecular chemical reaction one molecule at a time. More specifically, we have imaged a single O_2 molecule on the Pt(111) surface at low temperature, precisely positioned the STM tip above the molecule, dissociated the molecule with tunneling electrons from the STM tip without perturbing neighboring molecules, and imaged the two oxygen atom products. Because these experiments involve electrons tunneling from the outermost tip atom to the molecule of interest under the tip, excitations induced by the tunneling current are confined to only this molecule (dimensions of order 1 Å). This also allows the determination of the precise moment of dissociation for each molecule studied by monitoring the sudden change in the tunneling current caused by dissociation. Through repetition of the experiment, we have determined the dissociation rate as a function of tunneling current and voltage and explain the rates using a general model for dissociation induced by intramolecular vibrational excitations via resonant inelastic electron tunneling. Our results demonstrate the concept of single-molecule chemistry ("angstro-chemistry") with atomic resolution in the initiation of the reaction and imaging of the reactants and products.

Experiments were conducted in ultrahigh vacuum conditions (base pressure 2×10^{-11} Torr) with the STM and sample suspended by springs inside a radiation shield bolted to the bottom of a continuous flow liquid He cryostat, providing sample temperatures from 30 to 300 K. The shield has a clamping screw for rapid STM cooling, a small hole for *in situ* dosing, and a door for sample-tip transfer. STM tips were made from polycrystalline tungsten wire. The Pt(111) surface was prepared by repeated cycles of Ne^+ sputtering, annealing at 800 K in 8×10^{-8} Torr of oxygen, followed by annealing at 1250 K.

Molecularly adsorbed oxygen on Pt(111) has not previously been studied by STM. However, two chemisorbed O_2 species have been identified by traditional methods [9], both with the O-O bond aligned parallel to the surface [10]. Dissociation of O_2 has been observed to result from heating to temperatures above 100 K [11], UV light irradiation [12], and electron bombardment [13]. In a recent STM study, pairs of oxygen atoms were observed after O_2 dosing of Pt(111) in the temperature range of 150 to 206 K [14] and interpreted as thermal dissociation products.

We find that at temperatures below 40 K, weakly bound physisorbed molecules led to unstable images. Between 40 and 70 K, or at high coverages, terraces were populated only with tightly packed clusters of molecules. Dosing above 95 K led to thermal dissociation. To eliminate the possibility of thermal dissociation, the surface was dosed to low coverage at 85 K and then cooled to 50 K. A large scale image of the surface prepared in this way is shown in Fig. 1(a). On the terraces there are clusters, one-dimensional chains, and isolated molecules. This area also has a number of closely spaced steps which are decorated with oxygen molecules. A close-up image of these molecules is shown in Fig. 1(c) with a grid fit to the platinum atoms on the top terrace. The molecules on

 0031-9007/97/78(23)/4410(4)$10.00

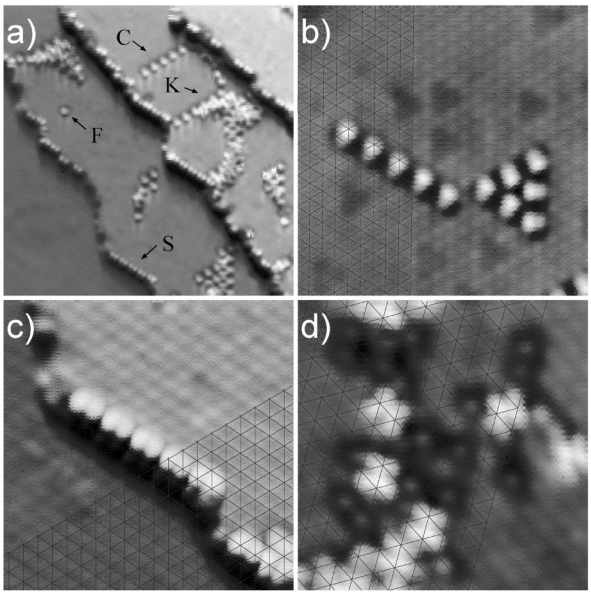

FIG. 1. (a) Large scale STM image of O_2 on the Pt(111) surface showing molecules at steps (labeled *S*), in clusters (*K*), chains (*C*), and in isolation (*F*). (b) Molecules on fcc sites (note grid fit to platinum lattice). All three orientations can be seen. (c) Molecules at a (111) step showing a grid fit to platinum lattice on upper terrace. (d) A cluster which has been partially dissociated with tunneling current in order to better show the individual molecules (four-leaf clovers) with a grid fit to the platinum lattice revealing adsorption on bridge sites. The distance between platinum atoms is 2.77 Å. Images are illuminated from above and were scanned at 50 mV sample bias and 5 nA tunneling current.

the upper terrace have two lobes visible with the midpoint at a bridge site. By extrapolating the grid to the lower terrace it is possible to distinguish fcc threefold sites from hcp threefold sites since hcp sites have an atom directly beneath them in the second layer. This analysis shows that molecules at the steps are adsorbed on (111) microfacets which have fcc sites nearer to the step edge than hcp sites. No molecules were found on steps with (100) microfacets. The ability to distinguish fcc and hcp sites is also important for assigning sites to the O_2 molecules and O atoms in the dissociation experiments discussed below. The molecules decorating the steps are stable up to about 150 K and are believed to be a previously undetected chemisorbed O_2 species.

Within the clusters on the terraces there are molecules [Fig. 1(d)] which the STM images as a "four-leaf clover" shape and are centered on bridge sites with a height of 0.5 Å above the platinum atoms. They have three possible orientations and a maximum local packing density of 0.5 ML in agreement with temperature programmed desorption (TPD) studies [15]. Based upon electron energy loss spectroscopy (EELS) [11] and near-edge x-ray absorption fine structure (NEXAFS) [16] experiments, these molecules are identified as a superoxo species with an energy loss peak of 860 cm^{-1}. The striking resemblance of these molecules with a π^* orbital suggests that the $\pi^*_{\|}$ resonance is the dominant contribution to the local density of states at the Fermi level for this chemisorbed state.

A third type of chemisorbed O_2 molecule found only at low coverages is also shown in Fig. 1(b) as well as in Fig. 2(a). This type of molecule is found at island perimeters, in chains with two lattice constants between molecules, and isolated on the surface. The coverage and dissociation temperature of 95 K indicate that this species is responsible for the 690 cm^{-1} peak in EELS experiments [11,17]. These molecules are centered on fcc threefold sites and have three possible orientations. In STM images, they have a "pear" shape with the bright lobe over a top site and the smaller, dimmer lobe over the opposite bridge site with a maximum height of about 0.2 Å above the platinum. We have been able to transform these pears into four-leaf clovers and vice versa by moving them with the STM tip. It should be noted that the adsorption sites determined for these species are different than those given previously in the literature [10,17].

The spatial selectivity of induced dissociation of two adjacent "pear-shaped" O_2 molecules by tunneling electrons is shown in Figs. 2(a)–2(d). The tip was precisely positioned (with an accuracy of about 1 Å) over the center of the molecule on the right and the feedback loop used to maintain constant tunneling current was turned off. A voltage pulse of duration 100 ms to 10 s was then applied, and the current was monitored. Figure 2(b) shows the current during a 0.3 V pulse with a sudden drop in

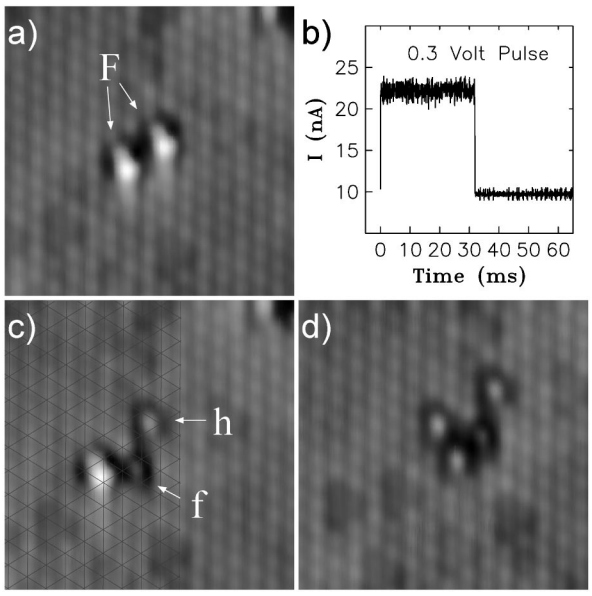

FIG. 2. (a) STM image of two adjacent pear shaped O_2 molecules on fcc sites. (b) Current during a 0.3 V pulse over the molecule on the right showing the moment of dissociation (step at $t \sim 30$ ms). (c) After pulse image with a grid fit to the platinum lattice showing one oxygen atom on an fcc and one on an hcp site along with the unperturbed neighboring molecule on an fcc site. (d) STM image taken after a second pulse with the tip centered over the molecule showing two additional oxygen atoms on hcp sites. Raw data images scanned at 25 mV sample bias and 5 nA tunneling current.

current indicating the moment of dissociation. A rescan of the same area in Fig. 2(c) shows the dissociated molecule with one oxygen atom on an fcc site and the other on an hcp site. The neighboring molecule (5.54 Å away) was unaffected by the pulse. By positioning the tip over this molecule and applying a second pulse, dissociation was observed with the two oxygen atoms on hcp sites. Atomic separations after dissociation by tunneling electrons were one to three lattice constants. These separations are comparable to those found for thermal dissociation [14], although atoms were found only on fcc sites after thermal dissociation. We therefore conclude that oxygen atoms on hcp sites are metastable at this temperature.

Hcp site atoms can be transferred to fcc sites as shown in Figs. 3(a)–3(d). Figure 3(a) shows a bridge-bound molecule, an impurity atom, a pair of oxygen atoms, and an isolated molecule on the surface along with several other molecules on fcc sites. After a pulse, Fig. 3(b) shows one oxygen atom on an hcp site and the other on an fcc site. The effect of a second pulse is shown in Fig. 3(c). The sudden rise in current (due to a greater tunneling conductance when the atom moves away) indicates the moment of atom transfer. A rescan of the same area in Fig. 3(d) showed both atoms on fcc sites.

The experiment depicted in Figs. 3(a) and 3(b) and Fig. 2(b) was repeated for 152 individual O_2 molecules on fcc sites completely isolated or near an impurity to determine the dissociation rate as a function of current and voltage. By averaging dissociation times for a given voltage and current, the characteristic time constant and rate were determined. No statistically significant difference in rates was found for a molecule near an impurity atom and a molecule completely isolated on the terrace. As shown in Fig. 4, fits to the data yield rates proportional to $I^{0.8\pm0.2}$, $I^{1.8\pm0.2}$, and $I^{2.9\pm0.3}$ for 0.4, 0.3, and 0.2 V pulses, respectively. Desorption of O_2 molecules on fcc sites by the tunneling current was not observed. Pulses applied to bridge-bound molecules could induce either the dissociation or the disappearance (presumably desorption) of the molecule while pulses applied to step-bound molecules always led to their disappearance.

The measured power-law dependence of the dissociation rate, R_d, on the tunneling current, I, $R_d \propto I^N$, and the magnitudes of R_d are explained using a model for bond breaking by inelastic electron tunneling through an adsorbate-induced resonance. As presented schematically in Fig. 5, this model is similar to the one used to explain femtosecond laser-induced surface chemistry [18] and represents a unification of previous models for tip-induced bond breaking experiments [5,6] either by multiple single-step excitations [19–21] or by single multiple-step excitations [22]. The potential energy well for the intramolecular bond coordinate is modeled by a truncated harmonic oscillator with energy levels $E(n)$. The dissociation dynamics of the molecule is described by a Pauli master equation for the transitions among the various levels of the oscillator [18–20,23]. The vibrational energy, $\hbar\omega =$ 87 meV (690 cm^{-1}), is taken from experiments [11,12]. The bond is assumed to break promptly as soon as its vibrational excitation reaches the "level" n_c. We have chosen five vibrational states within the potential well and $E(n_c) - E(n = 0) = 0.38$ eV, which corresponds to an energy barrier, E_{dis}, in the range of 0.35 to 0.38 eV. As shown in Fig. 5(b), the electron tunneling and the

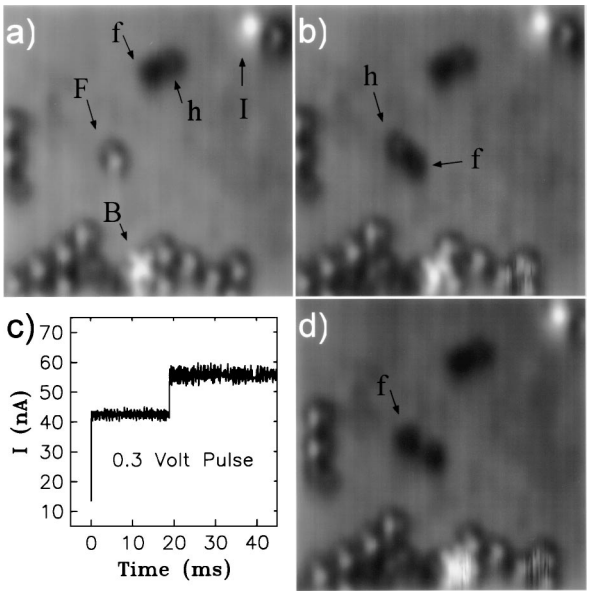

FIG. 3. (a) STM image of an isolated O_2 molecule on an fcc site (labeled F), an oxygen molecule on a bridge site (B), a dissociated pair of O atoms (f and h), and an impurity atom (I). (b) STM image after the pulse showing one fcc (f) and one hcp (h) site O atoms. (c) Current trace during a 0.3 V pulse showing the moment of atom transfer (step at $t \sim 20$ ms). (d) STM image after a second pulse showing both atoms on fcc sites. Raw data images scanned at 25 mV sample bias and 10 nA tunneling current.

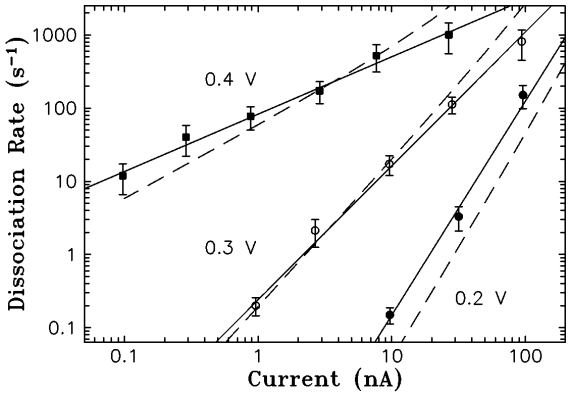

FIG. 4. Dissociation rate, R_d, as a function of tunneling current, I, for various applied biases. The solid lines are least squares fits to the data and correspond to power laws, $R_d \propto I^N$, where $N = 0.8 \pm 0.2, 1.8 \pm 0.2$, and 2.9 ± 0.3 for sample biases of 0.4, 0.3, and 0.2 V with respect to the tip, respectively. Results from the theoretical model (Fig. 5) are shown with dashed lines and have corresponding exponents of $N = 1.17, 2.07$, and 3.13, respectively.

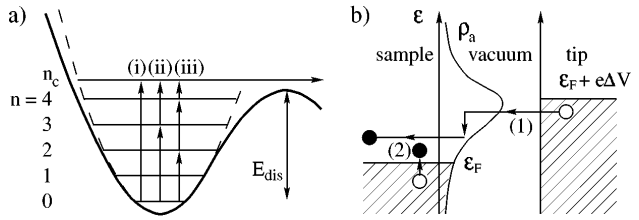

FIG. 5. Schematic picture of the model for bond breaking of O_2/Pt(111) by inelastic electron tunneling: (a) Potential energy well (solid line) for the intramolecular bond coordinate is modeled by a truncated harmonic oscillator (dashed line). The three sets of excitations among the levels in (a) represent typical transitions that lead to dissociation for the three applied biases ΔV; (i) 0.4, (ii) 0.3, and (iii) 0.2 V. (b) Inelastic electron tunneling to an adsorbate-induced resonance with density of states ρ_a induces vibrational excitations, (1), while electronic excitations within the substrate induces vibrational relaxations, (2).

electron-vibration coupling are assumed to be dominated by an adsorbate-induced resonance, such as the antibonding π^* of O_2 with density of states ρ_a. The resonance energy with respect to the Fermi level and the resonance width are both taken to be 1.0 eV which are consistent with x-ray absorption measurements [10,24]. The inelastic electron tunneling induces vibrational excitations, with a rate that is current dependent. The electron-vibrational coupling constant, $\lambda = 0.13$ eV, is the only free parameter that is fitted to the experimental data. There is a current-independent vibrational relaxation rate, $\gamma/\hbar$, from electronic excitations within the substrate; $\gamma = 2.4$ meV reproduces the infrared vibrational line shape [25].

Figure 4 shows that the calculated curves for R_d are in good agreement with the data. All three curves were generated from the same set of parameters given above. The values for N have a simple physical interpretation. For a bias of 0.4 V, $N \sim 1$ because the energy of a single tunneling electron is sufficient to excite the intramolecular mode above the dissociation barrier, E_{dis}. At a bias of 0.3 V, this energy is below E_{dis}, and energy transfers from two tunneling electrons are required to break the bond. Since the rate for each step in the dissociation process is proportional to the tunneling current, $N \sim 2$. Three electrons are required at a bias of 0.2 V because of the discrete level structure in the potential well [see Fig. 5(a)] and $N \sim 3$. The good agreement between the theoretical modeling and the data indicates that N should change over a narrow range of the bias voltage, reflecting the quantized nature of the vibrational levels. For 0.4 V bias, the single-step process [22] dominates over multiple-step processes because the vibrational relaxation rate, $\gamma/\hbar = 4 \times 10^{12}$ s^{-1}, is much larger than the maximum electron current, $I/e = 6 \times 10^{11}$ s^{-1}, in contrast to the conditions in the atomic switch [5,19,20].

These studies demonstrate our ability to manipulate matter on the atomic scale and with single bond precision. In future work, it should be possible to position chemical reactants into specific geometries before initiating individual bimolecular reactions to further probe chemical dynamics at the atomic level.

Support of this research by the National Science Foundation under Grant No. DMR-9417866, the Department of Energy under Grant No. DE-FG02-91ER14205, the Department of Education, the Swedish Natural-Science Research Council, and the Swedish Research Council for Engineering Sciences is gratefully acknowledged.

[1] R. P. Feynman, *Engineering and Science 1960* (Calif. Inst. of Technol., Pasadena, 1960), p. 22.
[2] G. Binnig and H. Rohrer, Sci. Am. **253**, No. 2, 40–46 (1985).
[3] J. A. Stroscio and D. M. Eigler, Science **254**, 1319 (1991); Ph. Avouris, Acc. Chem. Res. **28**, 95 (1995).
[4] D. M. Eigler and E. Schweizer, Nature (London) **344**, 524 (1990).
[5] D. M. Eigler, C. P. Lutz, and W. E. Rudge, Nature (London) **352**, 600 (1991).
[6] T.-C. Shen *et al.*, Science **268**, 1590 (1995).
[7] G. Dujardin, R. E. Walkup, and Ph. Avouris, Science **255**, 1232 (1992).
[8] R. Martel, Ph. Avouris, and I.-W. Lyo, Science **272**, 385 (1996).
[9] J. L. Gland, B. A. Sexton, and G. B. Fisher, Surf. Sci. **95**, 587 (1980).
[10] C. Puglia *et al.*, Surf. Sci. **342**, 119 (1995).
[11] N. R. Avery, Chem. Phys. Lett. **96**, 371 (1983).
[12] W. D. Mieher and W. Ho, J. Chem. Phys. **91**, 2755 (1989).
[13] T. M. Orlando *et al.*, J. Chem. Phys. **93**, 9197 (1990).
[14] J. Wintterlin, R. Schuster, and G. Ertl, Phys. Rev. Lett. **77**, 123 (1996).
[15] A. Winkler *et al.*, Surf. Sci. **201**, 419 (1988).
[16] D. A. Outka *et al.*, Phys. Rev. B **35**, 4119 (1987).
[17] H. Steininger, S. Lehwald, and H. Ibach, Surf. Sci. **123**, 1 (1982).
[18] S. Gao, D. G. Bush, and W. Ho, Surf. Sci. Lett. **344**, L1252 (1995); S. Gao, Phys. Rev. B **55**, 1876 (1997).
[19] S. Gao, M. Persson, and B. I. Lundqvist, Solid State Commun. **84**, 271 (1992); J. Electron. Spectrosc. Relat. Phenom. **64/65**, 665 (1993); Phys. Rev. B **55**, 4825 (1997).
[20] R. E. Walkup, D. M. Newns, and Ph. Avouris, Phys. Rev. B **48**, 1858 (1993).
[21] Ph. Avouris *et al.*, Surf. Sci. **363**, 368 (1996).
[22] G. P. Salam, M. Persson, and R. E. Palmer, Phys. Rev. B **49**, 10 655 (1994).
[23] J. W. Gadzuk, Phys. Rev. B **44**, 13 466 (1991).
[24] W. Wurth *et al.*, Phys. Rev. Lett. **65**, 2426 (1990).
[25] B. N. J. Persson, Chem. Phys. Lett. **139**, 457 (1987).